

# Magnetothermoelectric power of ferromagnetic thin films

M. S. ANWAR<sup>1,2</sup>, B. LACOSTE<sup>1,3</sup> and J. AARTS<sup>1</sup>

<sup>1</sup> *Kamerlingh Onnes Laboratory, Leiden University, P.O.Box 9504, 2300 RA Leiden, The Netherlands*

<sup>2</sup> *Quantum Materials Lab., Department of Physics, Kyoto University, Kyoto 606-8502, Japan*

<sup>3</sup> *SPINTEC, UMR CEA/CNRS/UJF/INPG, CEA/INAC, 17 Rue des Martyrs, 38054 Grenoble, France*

PACS 72.15.Jf –  
PACS 73.50.Lw –

**Abstract** –We compare the behavior of the magnetothermoelectric power (MTEP) in metallic ferromagnetic thin films of  $\text{Ni}_{80}\text{Fe}_{20}$  (Permalloy; Py), Co and  $\text{CrO}_2$  at temperatures in the range of 100 K to 400 K. In 25 nm thick Py films and 50 nm thick Co films both the anisotropic magnetoresistance (AMR) and MTEP show a relative change in resistance and thermoelectric power (TEP) of the order of 0.2% when the magnetic field is reversed, and in both cases there is no significant change in AMR or MTEP any more after the saturation field has been reached. Surprisingly, both Py and Co films have opposite MTEP behavior although both have the same sign for AMR and TEP. The data on 100 nm films of fully spin-polarized  $\text{CrO}_2$ , grown both on  $\text{TiO}_2$  and on sapphire, show a different picture. The MTEP behavior at low fields shows peaks similar to the AMR in these films, with variations up to 1%. With increasing field both the MR and the MTEP variations keeps growing, with MTEP showing relative changes of 1.5% with the thermal gradient along the  $b$ -axis and even 20% with the gradient along the  $c$ -axis, with an intermediate value of 3% for the film on sapphire. It appears that the low-field effects are due to magnetic domain switching, while the high-field effects are intrinsic to the electronic structure of  $\text{CrO}_2$ .

**Introduction.** – Electronic transport in ferromagnets is spin-dependent, which is the basis for e.g. anisotropic magnetoresistance (AMR), giant magnetoresistance (GMR) and tunneling magnetoresistance (TMR). Thermoelectric effects, although known since the nineteenth century, have been much less studied in conjunction with spin effects. In ferromagnets it is predicted that heat transport is spin-dependent, more precisely that thermoelectric power (TEP) is spin-dependent, opening the new field of Spin Caloritronics [1]. Recent experiments here are for example the Spin-Seebeck Effect (SSE) [2], TEP in multilayer nanowires [3], thermally induced spin torque in nonlocal lateral spin-valves [4] or the Spin Peltier effect [5]. More recently an equivalent to TMR for thermoelectric transport was observed, tunneling magnetothermoelectric power (TMTEP) [6], with a relative magnitude of the same order as TMR. In this paper we concentrate on the magnetic field dependence of the thermoelectric power (the magneto-thermoelectric power or MTEP). In particular, we study MTEP for two simple  $3d$  ferromagnets (Co and Py), and the correlated electron system  $\text{CrO}_2$ , which is fully spin-polarized, and

we compare MTEP behavior to the better known AMR behavior.

Theoretically, magnetoresistance and magnetothermoelectric power (MTEP) are not directly related. The intrinsic conductivity is proportional to the density of states (DOS) at the Fermi level, whereas the intrinsic TEP depends on the derivative of the DOS, through the derivative with respect to energy of the conductivity  $\sigma$ . The TEP, denoted with  $S$ , is given by [7],

$$S = -eL_oT \frac{\sigma'(\epsilon_F)}{\sigma(\epsilon_F)}, \quad (1)$$

which is known as Mott's Law for TEP [8]. Here,  $L_o$  is the Lorentz number, which is a universal quantity  $L_o = 2.45 \times 10^{-8} \text{W}\Omega\text{K}^{-2}$ , and  $\epsilon_F$  is the Fermi energy. This expression illustrates that TEP is linear in  $T$ , at least for diffusive electronic contribution. A  $T^3$  dependence term is added if the phonon drag phenomenon is also contributing to the TEP. In a ferromagnetic material magnon drag can contribute along with diffusive and phonon drag. The magnon drag part goes as  $T^{3/2}$  which

makes it difficult to differentiate the phonon and magnon contributions [9].

Equation 1 is valid for a homogeneous conductor having only one kind of carriers when variations of the mean free path ( $\lambda_e$ ) and relaxation time ( $\tau_e$ ) with respect to energy are negligible. A ferromagnet has different DOS at the Fermi level for spin up ( $N_{\uparrow}(\epsilon_F)$ ) and spin down electrons ( $N_{\downarrow}(\epsilon_F)$ ) so that Mott's Law can be written as [10],

$$S = -eL_oT \left\{ \frac{\sigma'_{\uparrow}(\epsilon_F)}{\sigma_{\uparrow}(\epsilon_F)} + \frac{\sigma'_{\downarrow}(\epsilon_F)}{\sigma_{\downarrow}(\epsilon_F)} \right\} = (S_{\uparrow} + S_{\downarrow}), \quad (2)$$

and still valid in situations when  $\lambda_e$  and  $\tau_e$  do not vary significantly. In inhomogeneous systems such as magnetic multilayer, or magnets in a domain state, this will be different. For instance, Piraux *et al.* [11] investigated the consequences of electron-magnon scattering in the framework of GMR, which is instructive to mention here. A spin down (up) electron of wave vector  $k$  can be scattered into a spin up (down) state with wave vector  $k' = k \pm q$  under creation (annihilation) of a magnon with wave vector  $q$ . The magnon energy  $E_q$  will transfer to or from the electron. This results in a maximum scattering rate for spin up electrons with energies below  $\epsilon_F$ , and spin down electrons with energies above. As a result the relaxation rate at  $\epsilon_F$  will have different signs and an opposite effect for both spin directions. As a result, the magnon scattering contribution to the thermopower is  $S_{\uparrow(\downarrow)}^m = \mp \frac{L_o}{k_B}$ , and we get,

$$S^m = -\frac{L_o}{k_B} \frac{N_{\uparrow}(\epsilon_F) - N_{\downarrow}(\epsilon_F)}{N_{\uparrow}(\epsilon_F) + N_{\downarrow}(\epsilon_F)}, \quad (3)$$

and therefore depends on the spin polarization. This contribution to the thermopower will go to zero for weak ferromagnets where the difference between the DOS for spin-up and spin-down is small. Otherwise, the difference for the different spin channels has consequences for the TEP in F/N multilayers when the magnetic configuration is changed from parallel to antiparallel.

Going from TEP to MTEP, the (direction of) magnetization becomes another parameter, and in particular magnetic domain formation can be expected to have an influence on the TEP and a relation to AMR. This question has been addressed for thin films of ferromagnetic semiconductor Mn-doped GaAs, where longitudinal and transverse MTEP was measured with in-plane applied magnetic field. The effect was found to be related to the AMR and Planar Hall effect (PHE) [12]. We studied MTEP in thin films of itinerant 3d (and partially spin polarized) ferromagnets, namely Co (50 nm thick) and Py (25 nm thick); and in 100 nm thick films of fully spin-polarized CrO<sub>2</sub> ferromagnetic metal. In all case we find that MTEP has a signature similar to AMR, although, somewhat surprisingly, the signs of both effects do not match completely. In CrO<sub>2</sub>, also the behavior of AMR and MTEP outside the

hysteresis loop is very similar. Quantitatively, the relative MTEP effects can be quite a bit larger than the AMR effects, as we will demonstrate.

**Experimentation.** – The Seebeck coefficient was measured using a home-made sample holder built on a puck which can be placed inside an automated measurement platform (a PPMS from Quantum Design). It consists of two copper blocks (1 cm<sup>3</sup>) separated by a thermally insulating plastic. The copper has a high thermal conductance, so the blocks are at a uniform temperature while a temperature gradient is produced between them. A small heater (maximum power of 5 W) is installed in the upper block. Its temperature is measured with a Pt-100 resistor and controlled with an external temperature controller. The temperature of the lower block is controlled by the set point of the PPMS, but the temperature was separately measured by a second Pt-100 resistor. The whole setup is covered with a stainless steel cup that isolates the sample holder from radiation loss and it helps to stabilize the temperature gradient. The measurements were done in a relatively low vacuum of 10<sup>-2</sup> mbar. A schematic of the sample holder is given in fig.1

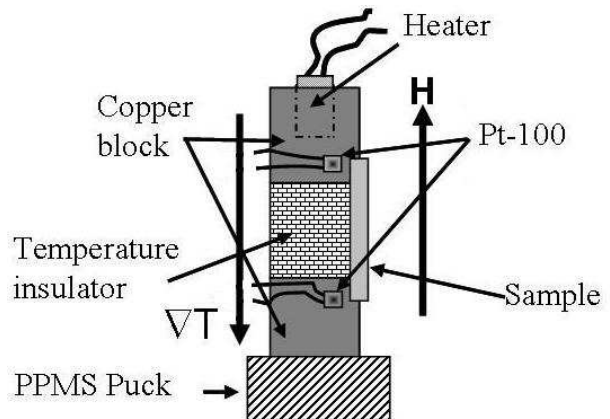


Figure 1: Schematic of thermal transport sample holder built on a PPMS puck. Two copper blocks are separated by a thermally insulating plastic. A heater is installed in the upper Cu block and two Pt-100 resistors are used to measure the temperature difference between the Cu blocks. The whole set up is covered with a stainless steel cap, not shown.

The samples consisted of thin films with an area of 10 × 10 mm<sup>2</sup>. The Py thin films with a thickness of 25 nm were deposited using dc sputtering in a UHV sputtering system, with a base pressure of 10<sup>-9</sup> mbar. The Co films with a thickness of 50 nm were deposited in a (Leybold) Z-400 RF sputtering system with a base pressure of 10<sup>-6</sup> mbar. Both Py and Co were deposited on sapphire substrates because of its better thermal conductivity. Thin films of CrO<sub>2</sub> of 100 nm thickness were deposited by Chemical Vapor Deposition (CVD) on both isostructural TiO<sub>2</sub>(100) and sapphire (1000) substrates. CrO<sub>2</sub> films grow epitaxially on TiO<sub>2</sub> in the form of rectangular grains aligned along

the  $c$ -axis but on sapphire the grain structure shows a six fold rotational symmetry coming from the hexagonal structure of the substrate. For details we refer to Ref. [13].

The Seebeck coefficient was recorded with reference to copper since Cu wires were connected at both ends of the film via pressed Indium. The potential difference was probed using a Nanovoltmeter (Keithley 218) in an open circuit geometry (zero charge current). A dynamic technique was utilized to measure TEM as function of temperature in which the temperature difference between hot and cold point was always 5 K, while the temperature of the cold point was increased by 10 K in each step. In this way hot point and cold point interchanged in each step between the temperature range of 100 - 400 K [14]. For the MTEP measurements, a larger temperature difference of 45 K was used in all cases.

**Results.** – To check the setup, TEP was measured for 100 nm thick thin films of Cu and Au, with reference to Cu at room temperature. In principle this should give a zero TEP on a Cu film, but we measured around  $0.5 \mu\text{V}$  at a temperature difference of 10 K, which gives a TEP of the order of  $0.05 \mu\text{V/K}$ . The small TEP validates the assumption that we can take Cu as a reference for the TEP measurements and also attest to the functioning of our home-built sample holder. The non-zero voltage can be attributed to the pressed Indium used to contact the Cu wires with the sample; also, the Cu wires may not have been connected strongly enough with the temperature bath, which can still generate some temperature difference between the voltage pads. TEP on Au thin film gives the value of  $-0.4 \mu\text{V/K}$  with reference to Cu. The absolute TEP of Au at 300 K is  $1.94 \mu\text{V/K}$ , whereas for Cu, it is  $1.84 \mu\text{V/K}$ , which makes TEP of Au in reference to Cu to be  $+0.1 \mu\text{V/K}$ . The sign change again points to the In, since the absolute TEP of In is around  $1.5 \mu\text{V/K}$  [15], giving a larger negative TEP in reference to Cu than Au.

Figure 2a shows the temperature dependent TEP of a 25 nm thick Py film deposited on a sapphire substrate. It shows roughly linear behavior with  $\text{TEP} = -7.8 \mu\text{V/K}$  at 300 K. It is a somewhat smaller value than the value reported in the literature,  $-20 \mu\text{V/K}$  [2] or  $-15 \mu\text{V/K}$ , [16]. The reasons for this difference can be the effect of an oxide layer on the film and its slightly different thickness [17].

Next, a magnetic field  $H \parallel \Delta T$  was applied and TEP measured. We use the absolute values of the TEP to define the MTEP, as follows:

$$\text{MTEP} = \frac{|TEP(H)| - |TEP_{extr}|}{|TEP_{extr}|} \quad (4)$$

where  $TEP_{extr}$  is the extremal value (maximum or minimum) of the TEP at some low field (mostly a peak at the coercive field). As a consequence, a positive relative change means an *increase* in TEP with field and vice versa. Figure 2b presents the TEP as a function of externally ap-

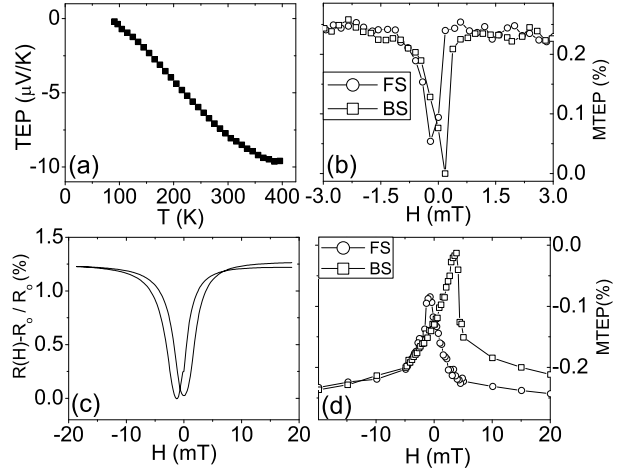


Figure 2: (a) Thermoelectric power (TEP) as a function of temperature for a 25 nm thick Py thin film in the temperature range of 100 - 400 K measured with a constant  $\Delta T$  of 5 K. (b) MTEP for the same film at  $\bar{T} = 178$  K and  $\Delta T = 45$  K, with the field applied along the temperature gradient. (c) AMR for the same Py film, measured at 4.2 K. (d) MTEP measurements for a 50 nm thick Co thin film measured at  $\bar{T} = 178$  K with  $\Delta T = 45$  K and the field applied along the temperature gradient. Note the difference in sign compared to the data on Py.

plied field in parallel configuration ( $\Delta T \parallel H$ ) on Py at an average temperature  $\bar{T} = 178$  K and  $\Delta T = 45$  K. Sharp peaks appear at 0.2 mT and -0.2 mT corresponding to the coercive fields. The TEP is higher in the saturation state and lower in a domain state with a relative change of 0.2%. Such a behavior of MTEP is similar to the positive AMR effect (lower resistance in domain state) in Py films, as shown in fig. 2c, measured at 4.2 K. The same effect is observed for a 50 nm thick Co thin film (see fig. 2d), where peaks appear at -0.7 mT and 3.8 mT. Note that for Co the TEP is *lower* in the saturation state and *higher* in the domain state, opposite to the films of Py, although Co and Py have the same sign of zero-field TEP and of AMR. The MTEP for both films saturates just as magnetization or AMR. The hysteretic behaviour of MTEP and the peaks around the coercive field reveal the direct connection of MTEP with the magnetization orientation in the films. The MTEP signal at around 200 K is almost the same in magnitude for both films.

The effect of magnetization on MTEP was also studied with a sample consisting of a bilayer ferromagnet of  $\text{Cu}_{41}\text{Ni}_{59}$  (50 nm)/Py (25 nm) deposited on a sapphire substrate.  $\text{Cu}_{41}\text{Ni}_{59}$  is a weak ferromagnet with a  $T_c$  of about 150 K. Figure 3a shows the data at  $\bar{T} = 185$  K and  $\Delta T = 30$  K, where two central sharp peaks appear corresponding to the domain switching in Py. The data recorded at  $\bar{T} = 125$  K, below the  $T_c$  of CuNi, show two more rather wide peaks besides the peaks of Py (see fig. 3b). These additional peaks appearing around 7 mT correspond to the coercive field of CuNi. It demonstrates a strong rela-

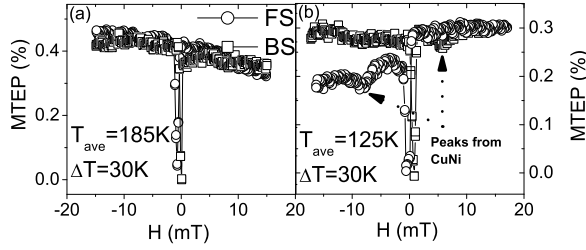


Figure 3: MTEP for a multilayer CuNi(50)/Py(25) film deposited on a sapphire substrate. (a) At  $\bar{T} = 185$  K, which is higher than Curie temperature of CuNi (150 K), when there are only two strong peaks corresponding coercive field of Py. (b) At lower temperature  $\bar{T} = 125$  K, other two peaks appeared corresponding to CuNi.

tion of MTEP to the magnetization and magnetic domain effects, similar to AMR.

Figure 4a shows the temperature dependent TEP for CrO<sub>2</sub> thin films deposited on sapphire and TiO<sub>2</sub> substrates, with the field and temperature gradient along the *c*-axis (easy axis) and the *b*-axis (hard axis). Figure 4b shows the temperature dependent resistivity data of these films for comparison. A room temperature value of  $-9 \mu\text{V/K}$  is measured for a CrO<sub>2</sub> film deposited on a sapphire substrate and the TEP decreases linearly with decreasing temperature, approaching zero at 100 K. However for the CrO<sub>2</sub> film deposited on TiO<sub>2</sub>, the TEP has a nonlinear dependence with respect to temperature for applied field along both the *c*-axis and the *b*-axis. The TEP along the *c*-axis changes sign at 265 K and has a room temperature value of  $-3 \mu\text{V/K}$ . Along the *b*-axis, CrO<sub>2</sub> has a negative TEP for the whole temperature range, with room temperature value of  $-23 \mu\text{V/K}$ , which is quite similar to the literature value of  $-25 \mu\text{V/K}$  [18], where the crystallographic axis is not mentioned.

Figure 4c presents the MTEP for a 100 nm thick CrO<sub>2</sub> thin film deposited on a sapphire substrate at  $\bar{T} = 178$  K and  $\Delta T = 45$  K and in parallel configuration. The TEP is maximum in the domain state and starts to decrease with the increase in field. Two strong peaks at 10 mT appear. They correspond to the peaks at coercive field also visible in AMR as shown in fig. 4d. For higher magnetic field, above 20 mT, the MTEP and AMR show the same field dependence in CrO<sub>2</sub> thin films. The relative change between maximum and minimum TEP at 200 K is about  $-3\%$ , which is 15 times larger than AMR signal which was recorded at 4.2 K.

Figure 5 shows the data for MTEP and AMR along both in-plane axes (the *c*-axis and the *b*-axis) for a 100 nm thick CrO<sub>2</sub> thin film deposited on a TiO<sub>2</sub> substrate. For MTEP measurements the magnetic field  $H$  and  $\Delta T$  are parallel to each other, as are field and current (100  $\mu\text{A}$ ) for the AMR measurements. Along the *c*-axis the MTEP data show two peaks at the coercive field. CrO<sub>2</sub> has neg-

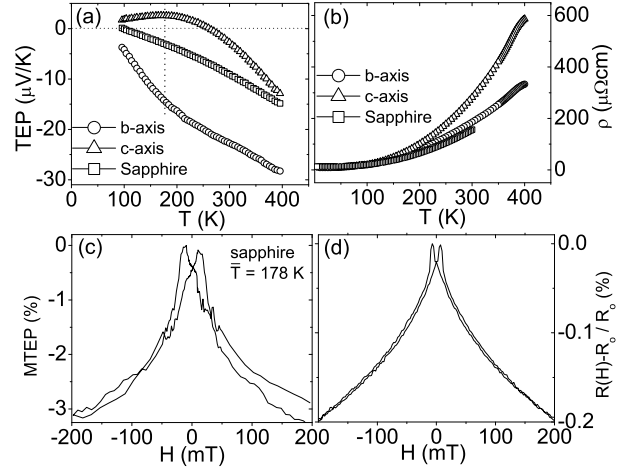


Figure 4: (a) Temperature dependent TEP measured in the temperature range of 100 - 400 K on 100 nm thick CrO<sub>2</sub> thin films deposited on sapphire ( $\square$ ) and TiO<sub>2</sub> substrate along the crystallographic *c*-axis ( $\triangle$ ) and the *b*-axis ( $\circ$ ). TEP changes the sign at 265 K along the *c*-axis. (b)  $\rho(T)$  for both films deposited on sapphire and TiO<sub>2</sub> substrates. (c) TEP as a function of externally applied field in parallel configuration for CrO<sub>2</sub> film deposited on sapphire at  $\bar{T} = 178$  K and  $\Delta T = 45$  K. (d) MR probed on same film at 4.2 K in parallel configuration ( $H \parallel I$ ).

ative relative change in TEP with field, so in the domain state the TEP is higher than in the saturation state. The peaks at coercive field are very sharp in both MTEP and AMR when the field is applied along the *c*-axis, whereas along the *b*-axis the peaks are less pronounced because of the smooth changes in the magnetic domains along the hard axis. These graphs show a very close correlation with MTEP and AMR or MR, which are both directly sensing the magnetization structure of the samples.

The relative change in MTEP along the *c*-axis is already 1% just in 50 mT at around 200 K. MTEP to higher fields shows more than 20% relative change, see fig. 6. Along the *b*-axis, the relative change in MTEP is 5 times larger than the MR in the range of 50 mT. The MTEP value is always much larger than the MR, regardless of the substrate used to grow the thin films of CrO<sub>2</sub>. In fig. 6, the saturation of MTEP at high fields, above 100 mT, is also obvious.

**Discussion.** — Our main purpose is the investigation of MTEP, but we can briefly comment on the temperature dependence of TEP in Py and CrO<sub>2</sub>. This is linear in Py between 100 K and 300 K (see fig. 2a), indicating that the electronic contribution dominates. For CrO<sub>2</sub>, TEP for films on TiO<sub>2</sub> exhibits non-linear temperature variations, as well as a difference between the *c*-axis and the *b*-axis. What is remarkable is the change in behavior around 200 K. Along the *b*-axis, TEP versus temperature curve shows a kink at around 200 K. Along the *c*-axis, the TEP slope vanishes around 200 K. We compare this behavior with that of the carrier concentration  $n(T)$  found via Hall Effect measurements, shown in fig. 7. The TEP change



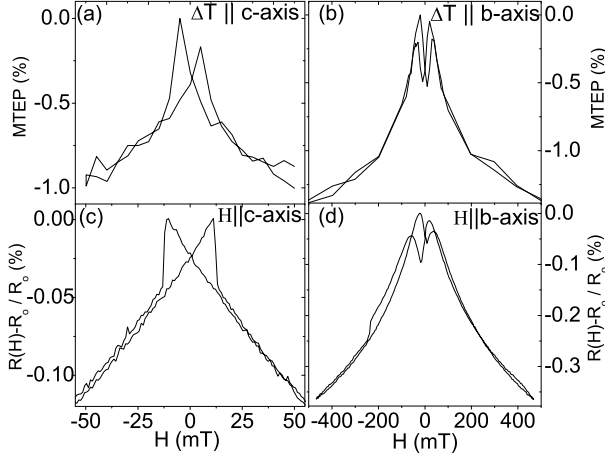


Figure 5: (a) MTEP measured at  $\bar{T} = 178$  K and  $\Delta T = 45$  K, along  $c$ -axis of a 100 nm thick  $\text{CrO}_2$  thin film deposited on  $\text{TiO}_2$  substrate. (b) MTEP along  $b$ -axis. (c) AMR measurements with a dc current of 100  $\mu\text{A}$  on same film along  $c$ -axis and (d) along  $b$ -axis. The peaks corresponding the coercive field are identical for both cases AMR and MTEP.

of slope (for both axes) at around 200 K corresponds to the temperature where the carrier concentration starts to decrease significantly. The films deposited on sapphire show a more linear relation. Since the change in slope is opposite for the  $b$ - and  $c$ -axis data, this looks like an average due to the random orientation of the grains in this film. The decrease in carrier concentration which is apparently reflected in the TEP has not been signalled before and will be discussed elsewhere [19]

Next, we focus on the variation of TEP with magnetic field. MTEP measurements presented here were all done with a temperature difference of around 45 K. The results for smaller temperature differences are similar. However for small temperature differences the noise level is larger, which is why only results for 45 K temperature difference are shown. The voltage difference measured is not exactly proportional to  $S(T)^2$  for large temperature difference, but rather  $V = \int_{T_1}^{T_2} S(T)dT$ , but this does not change the conclusions qualitatively. The message is that MTEP, like MR, is sensitive to the magnetic state of the sample. For Py (fig. 2b-c), the MTEP and MR curves show a very similar dependence. In the domain state the AMR shows a lower resistance (field || current), while MTEP shows a lower voltage (field || thermal gradient) than in the saturated state. Note that the AMR was measured at 4.2 K, since the effect at 200 K is much smaller. MTEP for Co shows similar behavior, except that the thermal voltage is now *increased* in the domain state as compared to the saturated state. It is well known that the AMR has the same sign for Co and Py [20], so this is a somewhat surprising result. It reinforces the notion that the difference of TEP for majority and minority spin electrons is not similar to the difference of resistance for

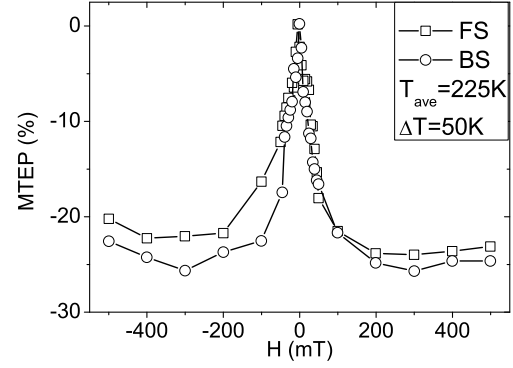


Figure 6: MTEP measurements along the  $c$ -axis of a 100 nm thick  $\text{CrO}_2$  film deposited on a  $\text{TiO}_2$  substrate at  $\bar{T} = 225$  K and  $\Delta T = 50$  K with hot point at 250 K. Maximum relative change in MTEP is of the order of 20%.

majority and minority spin electrons. The explanation will require more experiments.

For  $\text{CrO}_2$  the MTEP behavior faithfully mimics the MR as shown in fig. 5, both for the situations  $H \parallel c$  and  $H \parallel b$ . It is interesting to note that the MTEP variation is large, of the order of 1%, which is both significantly larger than the MTEP effect in Py, and than the AMR effects in general. The variations of MTEP is such that the thermopower is enhanced in the domain state, similar therefore to Co.

At high magnetic field, MTEP variations are also similar to MR, but much larger in amplitude. For the sapphire-based film the MTEP change at  $\bar{T} = 178$  K is 3% between 0 mT and 200 mT, for the  $\text{TiO}_2$ -based film ( $\Delta T \parallel c$ ) it is 1% up to 50 mT at the same temperature. An even larger effect is measured at  $\bar{T} = 225$  K, of 20% in a field of 200 mT (fig. 6). There is not yet much to connect to the experimental or theoretical literature. The comparison of Py and  $\text{CrO}_2$  indicates that the high spin polarization of  $\text{CrO}_2$  plays a role. The  $c$ -axis TEP shows a sign change around 250 K, and the large relative variation of the MTEP close to this temperature is possibly connected to this sign change. Still, all MTEP are an order of magnitude larger than the AMR for  $\text{CrO}_2$ . This may be connected to the granular nature of  $\text{CrO}_2$  thin films and the enhanced contribution to MTEP which can be expected due to inelastic scattering processes at grain boundaries.

In conclusion, we have presented a number of results of the behavior of the thermoelectric power in magnetic fields, measured on different ferromagnetic films. We compared them to the AMR behavior of the same films, and conclude that the magnetic domain state has a strong effect on the TEP, similar to what is found in AMR, and of relative magnitude which is significantly larger than AMR. The simple metals Co and Py show a straightforward vari-

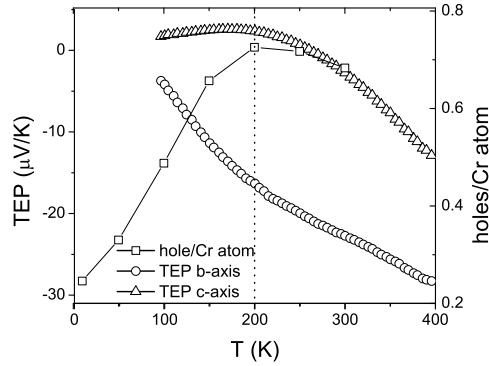


Figure 7: Temperature dependent TEP and carrier concentration of a 100 nm thick  $\text{CrO}_2$  film deposited on a  $\text{TiO}_2$  substrate. An obvious change in the slope of the TEP occurs around 200 K where the carrier concentration starts to decrease.

ation of TEP with temperature. The halfmetallic magnet  $\text{CrO}_2$  shows complex behavior, different along the different crystalline axes. Still, the MTEP behavior, also beyond the domain state, is similar to the AMR behavior.

\* \* \*

We are thankful to Santiago Serrano-Guisan for fruitful discussions. M.S.A. acknowledges the financial support of the Higher Education Commission (HEC) Pakistan.

## References

- [1] G. E. W. Bauer, A. H. MacDonald, and S. Maekawa, *Solid State Commun.* **150**, 459 (2010).
- [2] K. Uchida, S. Takahashi, K. Harii, J. Ieda, W. Koshibae, K. Ando, S. Maekawa, and E. Saitoh, *Nature* **455**, 778 (2008).
- [3] L. Gravier, S. Serrano-Guisan, F. Reuse and J. P. Ansermet, *Phys. Rev. B* **73**, 024419 (2006).
- [4] A. Slachter, F. L. Bakker, J-P. Adam and B. J. van Wees, *Nat. Phys.* **6**, 879 (2010).
- [5] J. Flipse, F. L. Bakker, A. Slachter, F. K. Dejene, and B. J. van Wees, *Nature Nanotech* **7**, 166 (2012).
- [6] N. Liebing, S. Serrano-Guisan, K. Rott, G. Reiss, J. Langer, B. Ocker, and H.W. Schumacher, *Phys. Rev. Lett.* **107**, 177201 (2011).
- [7] N. Mott and H. Jones, *The theory of the properties of metals and alloys*, Dover Publications, New York, 1958.
- [8] M. Jonson and G. D. Mahan, *Phys. Rev. B* **21**, 4223 (1980).
- [9] J. M. Ziman, *Principles of the theory of solids*, Cambridge University Press-London, 1964.
- [10] F. J. Blatt, P. A. Schroeder, C. L. Foiles and D. Greig, *Thermoelectric power in metals*, Plenum press New York and London, 1976.
- [11] L. Piraux, A. Fert, P. A. Schroeder, R. Loloee, and P. Etienne, *J. Magn. Magn. Mater.* **110**, L247 (1992).
- [12] Y. Pu, E. Johnston-Halperin, D. Awschalom, and J. Shi, *Phys. Rev. Lett.* **97**, 036601 (2006).
- [13] M. S. Anwar and J. Aarts, *Supercond. Sci. Technol.* **24**, 024016 (2011).
- [14] S. Compans, *Rev. Sci. Instrum.* **60**, 2715 (1989).
- [15] A. D. Caplin, C. K. Chiang, J. Tracy, and P. A. Schroeder, *Physica Status Solidi (a)* **26**, 497 (1974).
- [16] K. Uchida, T. Ota, K. Harii, S. Takahashi, S. Maekawa, Y. Fujikawa, and E. Saitoh, *Sol. St. Comm.* **150**, 524 (2010).
- [17] SCHEPIS R. and SCHRODER, K., *J. Magn. Magn. Mater.*, **104-107** (1992) 1757.
- [18] D. S. Chapin, J. A. Kafalas and J. M. Honig, *Jn. Phys. Chem.* **69**, 1402 (1965).
- [19] M. S. Anwar and J. Aarts, in preparation.
- [20] A. Fert and L. Piraux, *J. Magn. Magn. Mater.* **200**, 338 (1999).